GEOPHYSICAL RESEARCH LETTERS, VOL. 29, NO. 19, 1929, doi:10.1029/2002GL015609, 2002

Correction published 5 April 2003

Lidar backscatter to extinction, mass and area conversions for stratospheric aerosols based on midlatitude balloonborne size distribution measurements

Horst Jäger[1] and Terry Deshler[2]

Received 5 June 2002; revised 22 July 2002; accepted 23 July 2002; published 11 October 2002.

[1] Size distributions of the stratospheric sulfuric acid aerosol derived from balloonborne particle counter measurements from Laramie, Wyoming, are used to calculate ratios of particle extinction, mass, and surface area to particle backscatter, and the wavelength dependences of particle backscatter and extinction. These ratios may then be used to infer particle extinction, mass, and area from midlatitude lidar data in the spectral range 355 nm to 1064 nm for the time period 1991 to 1999. The conversions are defined in four height intervals from the tropopause to 30 km with a time resolution of four months. Results of conversions from earlier studies are included to span the time period 1979 to 1999. The eruptions of El Chichón (1982) and Pinatubo (1991) strongly influence these conversions. Extended background levels are observed prior to El Chichón and since about 1997. *INDEX TERMS:* 0305 Atmospheric Composition and Structure: Aerosols and particles (0345, 4801); 3360 Meteorology and Atmospheric Dynamics: Remote sensing; 3394 Meteorology and Atmospheric Dynamics: Instruments and techniques; 8409 Volcanology: Atmospheric effects (0370). **Citation:** Jäger, H., and T. Deshler, Lidar backscatter to extinction, mass and area conversions for stratospheric aerosols based on midlatitude balloonborne size distribution measurements, *Geophys. Res. Lett.*, *29*(19), 1929, doi:10.1029/2002GL015609, 2002.

1. Introduction

[2] The equatorial eruptions of El Chichón (1982) and Pinatubo (1991) perturbed the stratosphere of both hemispheres over many years. Further perturbations observed in the northern hemisphere since 1980 were caused by the eruptions of Mt. St. Helens (1980), Alaid (1981), and Ruiz (1985) and/or Nyamuragira (1986). Regular remote sensing of atmospheric particles by lidar is an excellent method to investigate the variability of the stratospheric sulfate aerosol, to detect and identify volcanic eruptions penetrating into the stratosphere, and to describe the decay of these perturbations to the background aerosol level. To extend lidar data to aid in quantifying and modeling the impact of stratospheric aerosols on the atmospheric radiation budget and on heterogeneous chemical processes requires in addition conversions from backscatter to wavelength dependent optical depth, and concentrations of mass and surface area of stratospheric particles.

[3] There have been several approaches to infer such information from e.g. sunphotometer measurements [*Russell et al.*, 1993], particle measurements aboard the ER-2 aircraft [*Brock et al.*, 1993], or SAGE II satellite extinction profiles [*Thomason and Osborn*, 1992] or multiwavelength lidar systems [*Ansmann et al.*, 1998]. However, many lidar systems in use are dependent on a single wavelength, and thus cannot produce these results. Here we describe a method to convert particle backscatter measurements, at the widely used lidar wavelength of 532 nm, to particle extinction, and particle mass and surface area. For a wider application of these results, wavelength dependences of backscatter and extinction in the range 355 to 1064 nm are offered, comprising the classical lidar wavelengths of conventional Nd:YAG and ruby lasers. This work is a continuation of earlier studies [*Jäger and Hofmann*, 1991, and *Jäger et al.*, 1995]. The method utilizes particle size and concentration data from balloon flights over Laramie, Wyoming. The geographic position of Laramie at 41°N makes the results applicable to northern midlatitudes. The work here extends *Jäger et al.* [1995] to cover 1991–1999, replacing the 1991–1993 results in *Jäger et al.* [1995]. Combining these results with *Jäger and Hofmann* [1991] allows us to cover the time period 1979–1999.

2. Data

[4] The method utilizes size distributions of stratospheric particles derived from monthly measurements with balloonborne optical particle counters which count and size individual particles. These counters measure number concentrations for particles with radii > 0.01 (total aerosol or condensation nuclei concentration), 0.15, and 0.25 μm. In addition concentations for radii > 0.95, 1.2, and 1.8 μm were measured January 82 to December 87. In 1989 some significant modifications were made to the original instrument. These resulted in measurements at eight sizes between 0.15 and 10.0 μm, May 1989–1992, and 0.15–2.0 μm, May 1992–November 1993. In November 1993 the number of sizes measured between 0.15 and 2.0 μm was increased to twelve, and this is the present configuration. The earlier instruments used for these measurements have been described by *Hofmann et al.* [1975], *Hofmann and Rosen* [1983], and the later instruments by *Hofmann and Deshler* [1991]. A description of the size distributions used to fit the aerosol concentration measurements and associated errors can be found in *Deshler et al.* [1993] and *Deshler and Oltmans* [1998].

[1]Institut für Meteorologie und Klimaforschung, Atmosphärische Umweltforschung (IMK-IFU), Forschungszentrum Karlsruhe GmbH, Garmisch-Partenkirchen, Germany.
[2]Department of Atmospheric Science, University of Wyoming, Laramie, Wyoming, USA.

0094-8276/02/2002GL015609$05.00

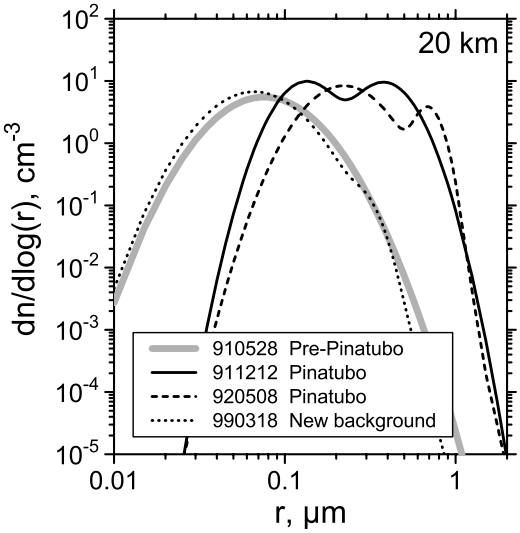

Figure 1. Aerosol size distributions derived from balloon-borne measurements above Laramie at an altitude of 20 km.

[5] Stratospheric background aerosols are characterized by lognormal size distributions peaking at radii <0.1 μm, which can be regarded as monomodal. In the case of high volcanic load the distribution is moved towards greater radii and can better be described by a bimodal lognormal distribution peaking at 0.05–0.4 μm (primary mode) and at approximately 0.4 to 0.8 μm (secondary mode). Figure 1 shows monomodal distributions from early 1991 (pre-Pinatubo) and 1999 (background) and two bimodal distributions describing the maximum Pinatubo load.

3. Calculation of Lidar Conversion Factors

[6] The calculation of particle extinction E (m^{-1}), particle mass concentration M (g m^{-3}), and particle surface area concentration S (μm^2 m^{-3}) from particle backscattering B (sr^{-1} m^{-1}) measured by lidar requires conversion factors E/B, M/B , and S/B, respectively. Mie calculations of light scattering and light extinction can be exercised for spherical particles with known refractive index, specific gravity, and size distribution. Except for a brief period after an eruption the stratospheric aerosol consists of aqueous liquid droplets with a 65–80% sulfuric acid content, depending on temperature [e.g., *Hofmann and Rosen*, 1983]. *Russell and Hamill* [1984] suggest a range of the refractive index of 1.44 to 1.45 and specific gravity values from 1.65 to 1.80 g cm^{-3}. These height dependent refractive index and specific gravity values are based on average midlatitude temperature and water vapor profiles. The imaginary part of the refractive index can be neglected because sulfuric acid droplets are almost nonabsorbing. This range of refractive index values excludes temperatures below −70°C, characteristic of polar winter conditions, and regions with elevated water vapor pressure close to the tropopause.

[7] The conversions are expressed as

$$E/B = \pi k^2 \int_0^\infty r^2 Q_e n(r)dr / \int_0^\infty I_b n(r)dr \quad m^{-1}\ sr\ m, \qquad (1)$$

$$M/B = 10^{-6} 4\pi\rho k^2/3 \int_0^\infty r^3 n(r)dr / \int_0^\infty I_b n(r)dr \quad g\ m^{-3}\ sr\ m, \qquad (2)$$

$$S/B = 10^{6} 4\pi k^2 \int_0^\infty r^2 n(r)dr / \int_0^\infty I_b n(r)dr \quad \mu m^2 m^{-3}\ sr\ m, \qquad (3)$$

where $k = 2\pi/\lambda$ at wavelength λ, r is the particle radius, Q_e is the Mie extinction efficiency function, I_b is the Mie backscatter intensity function, and n(r) is the differential particle size distribution. The conversion factors were calculated at 532 nm with a height resolution of 1 km, applying refractive indices of 1.44, 1.445, 1.45, and 1.45 and specific gravity values ρ of 1.65, 1.70, 1.75, and 1.80 in the height ranges tropopause (TP)–15, 15–20, 20–25, and 25–30 km, respectively.

[8] In addition wavelength exponents of particle backscatter (κb) and particle extinction (κe) were calculated at a refractive index of 1.45 to allow the conversion of backscatter or extinction coefficients determined at a wavelength λ_1 within the range of 355 nm to 1064 nm to any other wavelength λ_2 within this range:

$$B_{\lambda 2} = B_{\lambda 1}(\lambda_2/\lambda_1)^{\kappa b} \qquad (4)$$

$$E_{\lambda 2} = E_{\lambda 1}(\lambda_2/\lambda_1)^{\kappa e} \qquad (5)$$

[9] Conversion factors and wavelength exponents were averaged over the height ranges of TP–15, 15–20, 20–25, and 25–30 km and over the 4 month periods November–February, March–June, and July–October for each year.

[10] Two error sources affect these calculations, uncertainties with the particle counters and the standard deviation arising from averaging within the 5 km times 4 month intervals. The second of these reflects both variability due to changing air masses and measurement error. The air mass uncertainty will include deviations of refractive index from the midlatitude profile of *Russell and Hamill* [1984] due to water vapor and temperature uncertainties. Sizing uncertainties with the older particle counters used until 1987 were dealt with in *Jäger and Hofmann* [1991]. Uncertainty in the radii measured with the present instruments is on the order of 10% due to electro optical broadening of the measured light intensity.

[11] Slight deviations of the refractive index [*Palmer and Williams*, 1975] from a value of 1.45 over the spectral range used here are well within other uncertainties in the calculations of the wavelength exponents.

4. Results

[12] Volcanic aerosols caused decreases in E/B, M/B, and S/B (Figure 2) after El Chichón and Pinatubo, reaching a minimum in the year following each eruption. Extended background levels can be noticed prior to El Chichón and since about 1997. The recovery after El Chichón is slowed compared to after Pinatubo, probably due to the perturbations of Ruiz (1985) and/or Nyamuragira (1986), so that background conditions were not reached until just before the Pinatubo event [*Thomason et al.*, 1997].

[13] The wavelength exponents for particle backscatter (Figure 3) and extinction (Figure 4) were calculated for

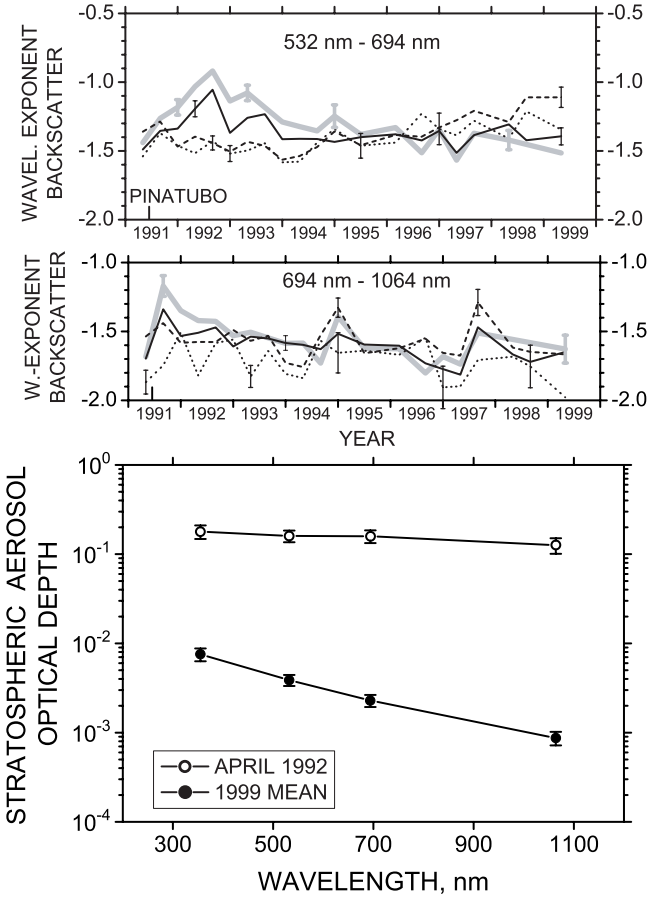

Figure 2. Particle extinction, mass, and surface area to backscatter conversion factors at 532 nm in four height ranges versus time including error margins.

three wavelength intervals 355–532 nm, 532–694 nm, and 694–1064 nm for the years 1991 to 1999. They increase after Pinatubo, with the extinction coefficient being more sensitive to the perturbation. The exponents also indicate background conditions beginning in 1997.

5. Discussion

[14] The time series of Figure 2 includes results from 3-channel (1970s) instruments transitioning (1980s) to multichannel instruments (1990s). The latter lead to more robust results due to better measurement of large particles. Considering these instrument changes, it is rather surprising that the results are comparable over many years with large changes in aerosol load.

[15] The change from background to volcanic levels is smallest with M/B and largest with S/B. During the three background periods, M/B shows similar results within the error margins, the E/B background has decreased since pre-El Chichón, and S/B has increased. *Jäger et al.* [1995] showed that M/B is relatively robust with respect to changing size distributions, whereas E/B and S/B are rather sensitive to the ratio of small to large particles within a size distribution. The reason for the decrease of E/B or increase of S/B at background levels could be a real change in the presence of larger particles since the late 1970s, or uncertainties in the determination of these larger particles. Further investigations into this question is limited by the lack of information for particles >0.25 μm in the early 3-channel measurements prior to 1982.

[16] Recall that, prior to El Chichón, the northern midlatitude stratosphere was perturbed by the eruptions of Mt. St. Helens (1980) and Alaid (1981); however, there was no significant influence on the conversion factors from these eruptions. This could be the result of not enough aerosol forming after these eruptions and/or simply not enough time to produce a significant impact on the large partice tail of the stratospheric aerosol size distribution prior to El Chichón.

[17] To identify the beginning of the new background period after the decay of the Pinatubo perturbation, parameters of size distributions were investigated to interpret the results shown in Figures 2–4. The widths of the distributions are not indicative. However, radii <0.08–0.1 μm in the primary mode and radii <0.4 μm in the secondary mode of the bimodal distributions indicate limits of a transition into a background situation. At both heights the mode 1 limit was reached in 1994 and the mode 2 limit in 1997. Total particle concentration returned to normal about two years after Pinatubo, but concentrations in the secondary mode remained elevated. A comparison with pre-Pinatubo conditions suggests that concentrations of large particles below 1% of the total particle number can be regarded as background. This has been the case since 1997.

6. Conclusions

[18] In situ aerosol size distributions can be used to calculate factors to convert lidar backscatter measurements into other geophysical quantities such as wavelength dependent aerosol extinction, mass and surface area. The

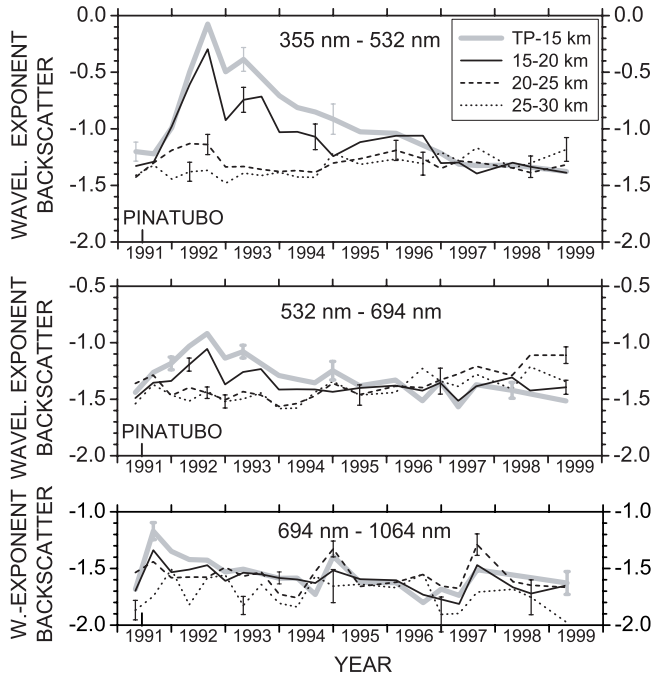

Figure 3. Wavelength exponents κb for particle backscatter between 355 nm and 1064 nm in four height ranges versus time including error margins.

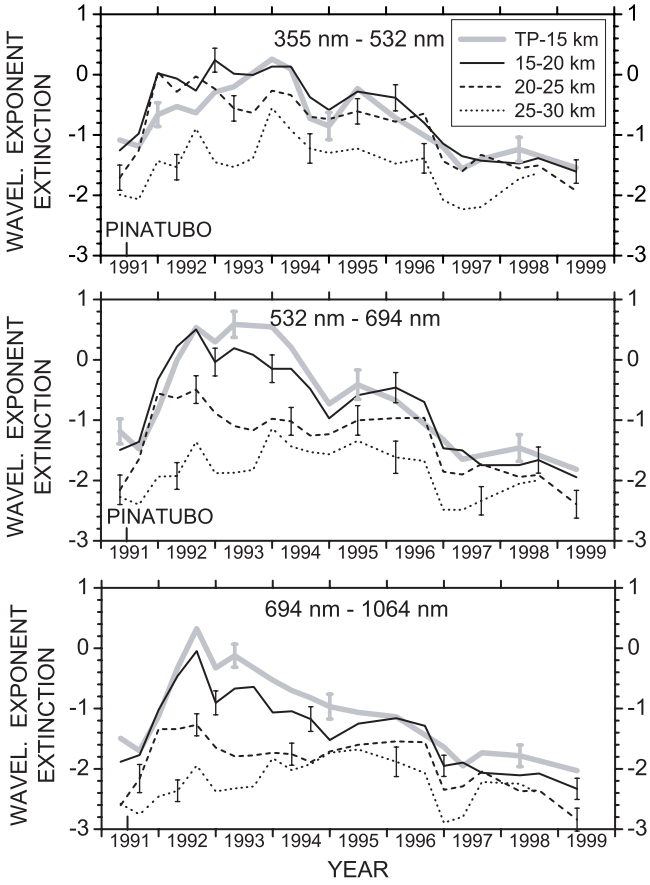

Figure 4. Wavelength exponents κe for particle extinction between 355 nm and 1064 nm in four height ranges versus time including error margins.

conversions are regarded valid for northern midlatitudes, but should be transferable to similar latitudes in the southern hemisphere in case of similar volcanic perturbations with a similar evolution of aerosol characteristics. The results are probably most useful to interpret lidar time series. The interpretation of individual lidar profiles or the intercomparison of lidar measurements requires caution because of airmass uncertainties.

[19] The results show that the interpretation of lidar backscatter from the stratosphere with respect to aerosol parameters might not be trivial after major volcanic eruptions and may be strongly influenced by low concentrations of large particles. Two factors play a role: the mass of volcanic sulfate aerosol forming in the stratosphere after an eruption, and the closeness of the eruption to the equator. Equatorial eruptions result in a longlasting perturbation usually of both hemispheres. The slow transport towards the polar sink of stratospheric air provides time for the formation of a significant fraction of large particles leading to effects observed over many years.

[20] **Acknowledgments.** The research at Garmisch-Partenkirchen has been supported by the German Bundesministerium für Bildung, Wissenschaft, Forschung und Technologie, and by the Commission of the European Union. H.J. is indebted to F. Homburg for computational assistance. The balloonborne measurements at Laramie have been supported by a number of agencies including the National Science Foundation, National Aeronautics and Space Administration, and Naval Research Laboratory.

References

Ansmann, A., I. Mattis, H. Jäger, and U. Wandinger, Stratospheric aerosol monitoring with lidar: Conventional backscatter versus Raman lidar observations of Pinatubo aerosol, *Contr. Atmos. Phys.*, *71*, 213–222, 1998.

Brock, C. A., H. H. Jonsson, J. C. Wilson, J. E. Dye, D. Baumgardner, S. Borrmann, M. C. Pitts, M. T. Osborn, R. J. DeCoursey, and D. C. Woods, Relationships between optical extinction, backscatter and aerosol surface and volume in the stratosphere following the eruption of Mt. Pinatubo, *Geophys. Res. Lett.*, *20*, 2555–2558, 1993.

Deshler, T., B. J. Johnson, and W. R. Rozier, Balloonborne measurements of Pinatubo aerosol during 1991 and 1992 at 41°N: Vertical profiles, size distribution, and volatility, *Geophys. Res. Lett.*, *20*, 1435–1438, 1993.

Deshler, T., and S. J. Oltmans, Vertical profiles of volcanic aerosol and polar stratospheric clouds above Kiruna, Sweden: Winters 1993 and 1995, *J. Atmos. Chem.*, *30*, 11–23, 1998.

Hofmann, D. J., J. M. Rosen, T. J. Pepi, and R. G. Pinnik, Stratospheric aerosol measurements I: Time variations at northern midlatitudes, *J. Atmos. Sci.*, *32*, 1446–1456, 1975.

Hofmann, D. J., and J. M. Rosen, Stratospheric sulfuric acid fraction and mass estimate for the 1982 volcanic eruption of El Chichón, *Geophys. Res. Lett.*, *10*, 313–316, 1983.

Hofmann, D. J., and T. Deshler, Stratospheric cloud observations during formation of the Antarctic ozone hole in 1989, *J. Geophys. Res.*, *96*, 2897–2912, 1991.

Jäger, H., and D. Hofmann, Midlatitude lidar backscatter to mass, area, and extinction conversion model based on in situ aerosol measurements from 1980 to 1987, *Appl. Opt.*, *30*, 127–138, 1991.

Jäger, H., T. Deshler, and D. J. Hofmann, Midlatitude lidar backscatter conversions based on balloonborne aerosol measurements, *Geophys. Res. Lett.*, *22*, 1727–1732, 1995.

Palmer, K. F., and D. Williams, Optical constants of sulfuric acid; application to the clouds of Venus?, *Appl. Opt.*, *14*, 208–219, 1975.

Russell, P. B., and P. Hamill, Spatial variation of stratospheric aerosol acidity and model refractive index: Implications of recent results, *J. Atmos. Sci.*, *41*, 1781–1790, 1984.

Russell, P. B., J. M. Livingston, E. G. Dutton, R. F. Pueschel, J. A. Reagan, T. E. DeFoor, M. A. Box, D. Allen, P. Pilewskie, B. M. Herman, S. A. Kinne, and D. J. Hofmann, Pinatubo and pre-Pinatubo optical-depth spectra: Mauna Loa Measurements, comparisons, inferred particle size distributions, radiative effects, and relationship to lidar data, *J. Geophys. Res.*, *98*, 22,969–22,985, 1993.

Thomason, L. W., and M. T. Osborn, Lidar conversion parameters derived from SAGE II extinction measurements, *Geophys. Res. Lett.*, *19*, 1655–1658, 1992.

Thomason, L. W., G. S. Kent, C. R. Trepte, and L. R. Poole, A comparison of the stratospheric aerosol background periods of 1979 and 1989–1991, *J. Geophys. Res.*, *102*, 3611–3616, 1997.

H. Jäger, Institut für Meteorologie und Klimaforschung, Atmosphärische Umweltforschung (IMK-IFU), Forschungszentrum Karlsruhe GmbH, D-82467 Garmisch-Partenkirchen, Germany. (horst.jaeger@imk.fzk.de)

T. Deshler, Department of Atmospheric Science, University of Wyoming, Laramie, WY 82071, USA. (deshler@uwyo.edu)